


A new small enantiornithine bird from the Jehol Biota, with implications for early evolution of avian skull morphology

Min Wang, Han Hu & Zhiheng Li


To cite this article: Min Wang, Han Hu & Zhiheng Li (2016) A new small enantiornithine bird from the Jehol Biota, with implications for early evolution of avian skull morphology, *Journal of Systematic Palaeontology*, 14:6, 481-497, DOI: [10.1080/14772019.2015.1073801](https://doi.org/10.1080/14772019.2015.1073801)

To link to this article: <http://dx.doi.org/10.1080/14772019.2015.1073801>

 View supplementary material [↗](#)

 Published online: 21 Aug 2015.

 Submit your article to this journal [↗](#)

 Article views: 314

 View related articles [↗](#)

 View Crossmark data [↗](#)

 Citing articles: 7 View citing articles [↗](#)

A new small enantiornithine bird from the Jehol Biota, with implications for early evolution of avian skull morphology

Min Wang ^{a*}, Han Hu ^a and Zhiheng Li^b

^aKey Laboratory of Vertebrate Evolution and Human Origins of Chinese Academy of Sciences, Institute of Vertebrate Paleontology and Paleoanthropology, Chinese Academy of Sciences, 142 Xizhimenwai Street, Beijing 100044, China; ^bDepartment of Geological Sciences, Jackson School of Geosciences, The University of Texas at Austin, 1 University Station C1100, Austin, Texas, 78712, USA

(Received 12 May 2015; accepted 11 June 2015; published online 21 August 2015)

Enantiornithes is the most diverse Mesozoic avian clade. Approximately half of the known global diversity of Enantiornithes is from the Early Cretaceous Jehol Biota of China. The Jehol enantiornithines are usually articulated and complete, but the bones are overlain by each other and preserved in two dimensions, severely limiting the number of cranial characters that can be recognized. Here we describe a new enantiornithine bird, *Pterygornis dapingfangensis* gen. et sp. nov., from the Jehol Biota. The new taxon has a unique sternal morphology with an external rostral spine and a pair of craniolateral processes. Phylogenetic analysis resolves the new taxon in a derived position within Enantiornithes. The specimen is disarticulated with several exceptionally well-preserved cranial bones, including the jugal and quadratojugal, morphologies of which remain poorly understood for enantiornithines. Our results indicate that the quadratojugal is an inverted L-shaped element, morphologically similar to that of more basal birds *Archaeopteryx bavarica*, *Jeholornis prima*, *Confuciusornis sanctus* and *Sapeornis chaoyangensis*. Our findings also illustrate that the quadratojugal underwent large modifications with the reduction of the caudoventral and squamosal processes sequentially during early avian evolution, contributing to the refinement of the cranial kinesis in early birds.

<http://zoobank.org/urn:lsid:zoobank.org:pub:384D11F5-1CD3-4447-B01E-58D320B42D49>

Keywords: Aves; Enantiornithes; jugal; Mesozoic; quadratojugal

Introduction

Over the last three decades, the Early Cretaceous Jehol Biota of China has yielded numerous and exceptionally well-preserved vertebrate fossils, making it an important Mesozoic lagerstätte for deciphering the evolution of diverse terrestrial vertebrate groups, particularly the early birds (Zhou *et al.* 2003; Benton *et al.* 2008; Zhou 2014). Currently, more than 40 avian species have been named from the Jehol Biota, spanning the whole spectrum of major Mesozoic avian clades (Zhou & Zhang 2006a; Zhou & Wang 2010). The Jehol bird-bearing deposits consist of, in ascending order, the Huajiying, Yixian and Jiufotang formations, which capture snapshots of over 10 million years of early avian history (130.7–120.0 Ma; Zhou *et al.* 2003; Jin *et al.* 2008; Pan *et al.* 2013). The large number of complete skeletons, some of which preserve feathers and in rare cases the traces of soft tissues, have added significantly to our knowledge about various aspects of early avian evolution, including morphology, biology, ontogeny and phylogeny (Zhang *et al.* 2006; Zheng *et al.* 2011, 2012, 2013, 2014; O'Connor *et al.*

2013a). More than half of the named Jehol birds are referred to Enantiornithes, which constitutes the sister group to Ornithuromorpha – the clade giving rise to all living birds (Zhou & Wang 2010; Wang *et al.* 2015). Enantiornithes is the most speciose and successful Mesozoic avian clade with worldwide distributions (Chiappe & Walker 2002; Longrich *et al.* 2011). The oldest record of this clade is from the Huajiying Formation (130.7 Ma; He *et al.* 2006; Jin *et al.* 2008), represented by *Protopteryx fengningensis* Zhang & Zhou, 2000 and *Eopengornis martini* Wang, O'Connor, Zheng, Wang, Hu & Zhou, 2014.

The Jehol birds are usually complete and articulated, but compressed in two dimensions. Consequently, key features regarding some skeletal elements, particularly the gracile skull bones, are obscured by crushed and overlying elements. Here we report a new enantiornithine bird from the Jiufotang Formation near Dapingfang Town, Chaoyang Country, in Liaoning Province, northeastern China. Although incomplete, the skeleton is disarticulated and several cranial elements are exquisitely well preserved in their entirety, providing morphological information that had previously been poorly understood.

*Corresponding author. Email: wangmin@ivpp.ac.cn

Methods

Institutional abbreviations

CAGS-IG: Chinese Academy of Geological Sciences, Institute of Geology, Beijing, China; **CNU:** Capital Normal University, Beijing, China; **LP:** Institut d'Estudis Ilerdencs, Lleida, Spain; **IVPP:** Institute of Vertebrate Paleontology and Paleoanthropology, Beijing, China; **STM:** Shandong Tianyu Museum of Nature, Shandong, China.

Phylogenetic analysis

A phylogenetic analysis was performed using the data matrix modified from Wang *et al.* (2014c). In addition to the new taxon, four recently described enantiornithines and basal ornithuromorphs were added: *Eopengornis martini* (STM24-1), *Piscivoravis lii* (IVPP V17078) and *Iteravis hunchzemeyeri* (IVPP V18958) were scored from their holotypes; and the character scorings for *Dunhuangia cuii* are after Wang *et al.* (2015). *Rahonavis ostromi* was removed from the matrix, because recent studies have indicated it was a dromaeosaurid rather than a bird (Norell *et al.* 2006; Turner *et al.* 2007). The modified data matrix consists of 60 taxa and 262 morphological characters (see Online Supplementary Material). The phylogenetic analysis was conducted using the TNT software package (Goloboff *et al.* 2008), with the following settings: space for 10,000 trees was set in the memory as the maxtrees; all characters were equally weighted, and 33 characters were treated ordered as in Wang *et al.* (2014c); an unconstrained heuristic search starting with Wagner trees was used; 1000 replicates of random stepwise addition (branch swapping: tree–bisection–reconnection, TBR) were performed and 10 trees were kept at each step; branches were collapsed to create polytomies if the minimum branch length equalled zero; Bremer and bootstrap values were calculated as indices of support; Bremer values were calculated by using Bremer scripts embedded in TNT; and the bootstrap value was retained by 1000 replicates using the same setting in the primary search.

Systematic palaeontology

Class *Aves* Linnaeus, 1758
 Ornithothoraces Chiappe, 1995
 Enantiornithes Walker, 1981
 Genus *Pterygornis* gen. nov.

Type species. *Pterygornis dapingfangensis* sp. nov.

Diagnosis. As for the type and only species.

Derivation of name. The genus name is derived from the Latin word 'pteryg' (wing), intended to reflect its unique

wings with fully ankylosed alular and major metacarpus, which distinguishes it from other known Early Cretaceous enantiornithines and suggests refined flight capability.

Pterygornis dapingfangensis sp. nov.
 (Figs 1–7)

Holotype. IVPP V20729, disarticulated and incomplete skeleton, representing an adult individual based on the complete fusion of the compound bones (Fig. 1; Table 1).

Derivation of name. The species name refers to the town of Dapingfang, where the fossil was collected.

Occurrence and age. Dapingfang Town, Chaoyang Country, Liaoning Province, northeastern China; Lower Cretaceous, Jiufotang Formation (He *et al.* 2004).

Diagnosis. A small, sparrow-sized enantiornithine, distinguishable from other enantiornithines by the combination of the following morphologies: surangular with rostroventrally sloping rostral margin, in contrast to the rostrorodorsal condition amongst other enantiornithines; omal half shaft of coracoid curved medially; sternum bearing an external rostral spine and a pair of cranio-lateral processes, both features absent in most other enantiornithines, e.g. *Eoenantiornis buhleri*, *Vescornis hebeiensis* and *Cathayornis yandica*; alular and major metacarpals fused with each other, a feature unknown in other Early Cretaceous enantiornithines; and trochlea of metatarsal II with well-formed ginglymoid articulation and a wide articular furrow on its planar surface.

Anatomical description

Anatomical terminology primarily follows Baumel & Witmer (1993), using English equivalents of the Latin terms. For structures not assigned preferred names therein, this paper follows Howard (1929).

Skull

Only the right maxilla is preserved, and is in medial view. The preserved jugal process is longer than the premaxillary process (Fig. 1). The dorsal process is caudodorsally directed and is craniocaudally compressed. A single tooth is preserved *in situ* in the premaxillary process and it is inclined rostrally. Caudally, a concavity may have represented an alveolus. A fragment carrying one tooth is preserved close to the maxilla, but the poor preservation precludes determination of its identity. The nasals are unfused medially; the bone is broad and tapers caudally, with a short maxillary process and an elongated premaxillary process. As in *Eoenantiornis buhleri* (Zhou *et al.*



Figure 1. Photograph of the holotype of *Pterygornis dapingfangensis* gen. et sp. nov. (IVPP V20729).

2005), the maxillary and premaxillary processes define a broad concave rostral notch, defining the caudodorsal margin of the external naris. The lacrimal is T-shaped, with the descending ramus longer and stouter than either the rostral or the caudal ramus. The rostral and caudal rami are rostroventrally and caudodorsally orientated, respectively. The dorsal margin of the lacrimal is nearly straight, lacking the concavity reported in some enantiornithines, including *Pengornis houii*, *Longsunguis kurochkini* and *Parabohaiornis martini* (O'Connor & Chiappe 2011; Wang *et al.* 2014c). Both jugals are preserved, and the bones are slender and rod-like (Figs 1, 3). The ventral margin of the maxillary process of the jugal slopes rostr dorsally as it extends rostrally, reminiscent of the morphology in *Bohaiornis guoi*, *L. kurochkini* and *Enantiornithes* indet. LP4450. As in *Cathayornis yandica* and *B. guoi* (Wang *et al.* 2014c; Wang & Liu 2015), the

caudal end of the jugal curves dorsally and tapers to a pointed tip. In contrast, the jugal is forked caudally with postorbital (ascending) and quadratojugal processes as in some enantiornithines, including *Shenqiornis mengi*, *L. kurochkini* and *Enantiornithes* indet. LP4450 (Sanz *et al.* 1997; O'Connor & Chiappe 2011; Wang *et al.* 2014c). Two delicate and L-shaped bones are interpreted as the quadratojugals (Fig. 3). Despite the fact that numerous specimens have been discovered, little is known about the morphology of this delicate element for enantiornithines. The quadratojugal has been described in the non-ornithothoracine birds *Archaeopteryx bavarica*, *Sapeornis chaoyangensis*, *Confuciusornis sanctus* and the basal ornithuromorph *Archaeorhynchus spathula* (Elzanowski & Wellnhofer 1996; Martin *et al.* 1998; Zhou & Zhang 2003, 2006b). In IVPP V20729, the quadratojugal resembles the morphology of the aforementioned taxa in that

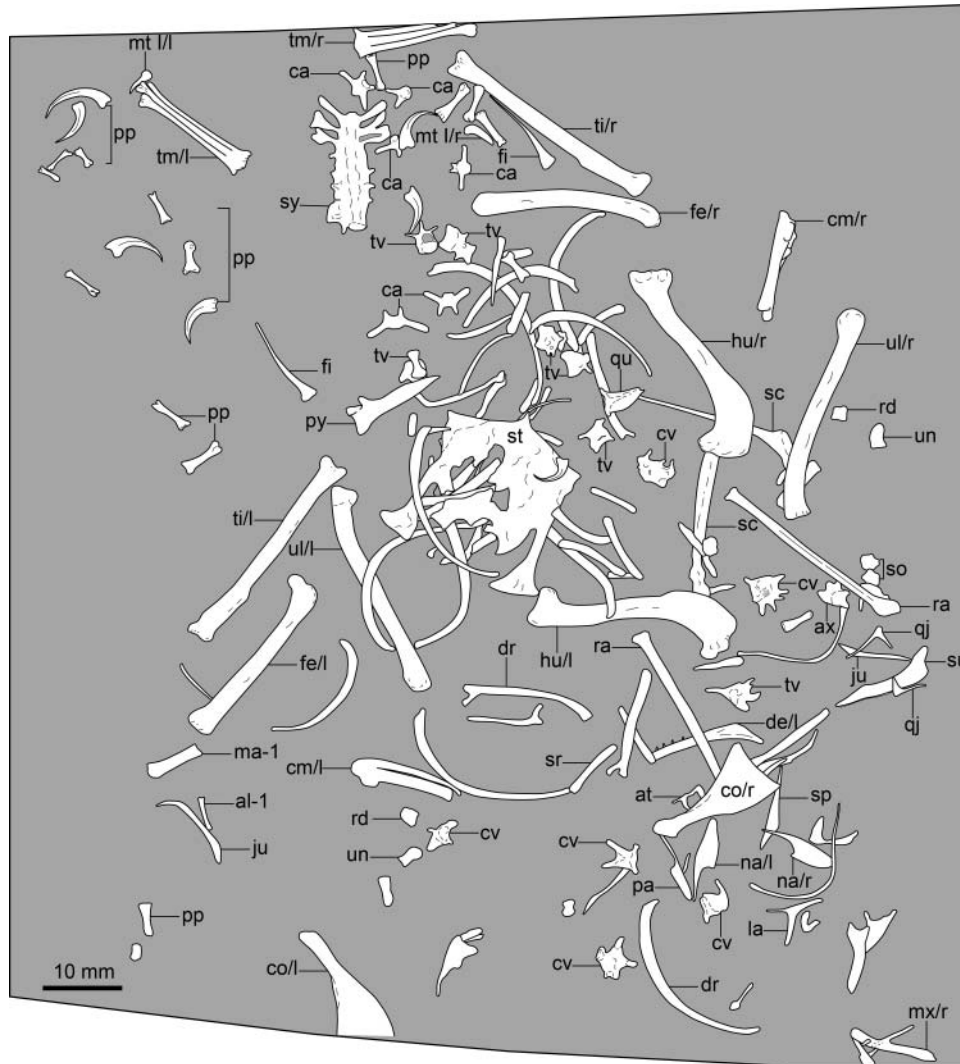


Figure 2. Interpretative line drawing of the holotype of *Pterygornis dapingfangensis* gen. et sp. nov. (IVPP V20729). Abbreviations: al-1, the first phalanx of alular digit; at, atlas; ax, axis; ca, caudal vertebra; cm, carpometacarpus; co, coracoid; cv, cervical vertebra; de, dentary; dr, dorsal rib; fe, femur; fi, fibula; hu, humerus; ju, jugal; la, lacrimal; ma-1, the first phalanx of major digit; mx, maxilla; mt I, metatarsal I; na, nasal; pa, palatine; pp, pedal phalanx; py, pygostyle; qj, quadratojugal; qu, quadrate; ra, radius; rd, radiale; sc, scapula; so, scleral ossicle; sp, splenial; sr, sternal rib; st, sternum; su, surangular; sy, synsacrum; ti, tibiotarsus; tm, tarsometatarsus; tv, thoracic vertebra; ul, ulna; un, ulnare; l, left side; r, right side.

the bone is an inverted L-shape with jugal and squamosal processes, but it is more delicate. These two processes define an acute angle approaching 90°. The slender jugal process is rod-like, and weakly tapers along its length. The squamosal process is shorter and tapers dorsally. The caudal end of the quadratojugal weakly protrudes caudally rather than forming a distinct process as in dromaeosaurids, in which this bone is shaped like an inverted T (Paul 1988; Xu & Wu 2001). The right quadrate is exposed in rostral view (Fig. 3). The orbital process is broken but leaves its base along the entire height of the quadrate. The otic process tapers dorsally. Although the dorsal tip is broken, the otic process is unlikely differentiated into the prootic and squamosal capitulum as present in Neornithes

(Baumel & Witmer 1993), given that its preserved dorsal end is considerably narrow. As in *S. mengi*, the madibular process is bicondylar and the medial condyle is larger than the lateral condyle (O'Connor & Chiappe 2011). Unlike the condition in *S. mengi* and *P. houi* (Zhou *et al.* 2008; O'Connor & Chiappe 2011), the quadrate is imperforated by a foramen.

Only the left dentary is preserved in lateral view (Fig. 1). The bone is typically enantiornithine in that the dorsal margin is straight and the caudal end slopes caudoventrally (O'Connor & Chiappe 2011). Four teeth are visible; however, the rostral end and the portion caudal to the preserved fourth tooth are overlain by the rib and radius, preventing the observation of additional teeth if they were present.

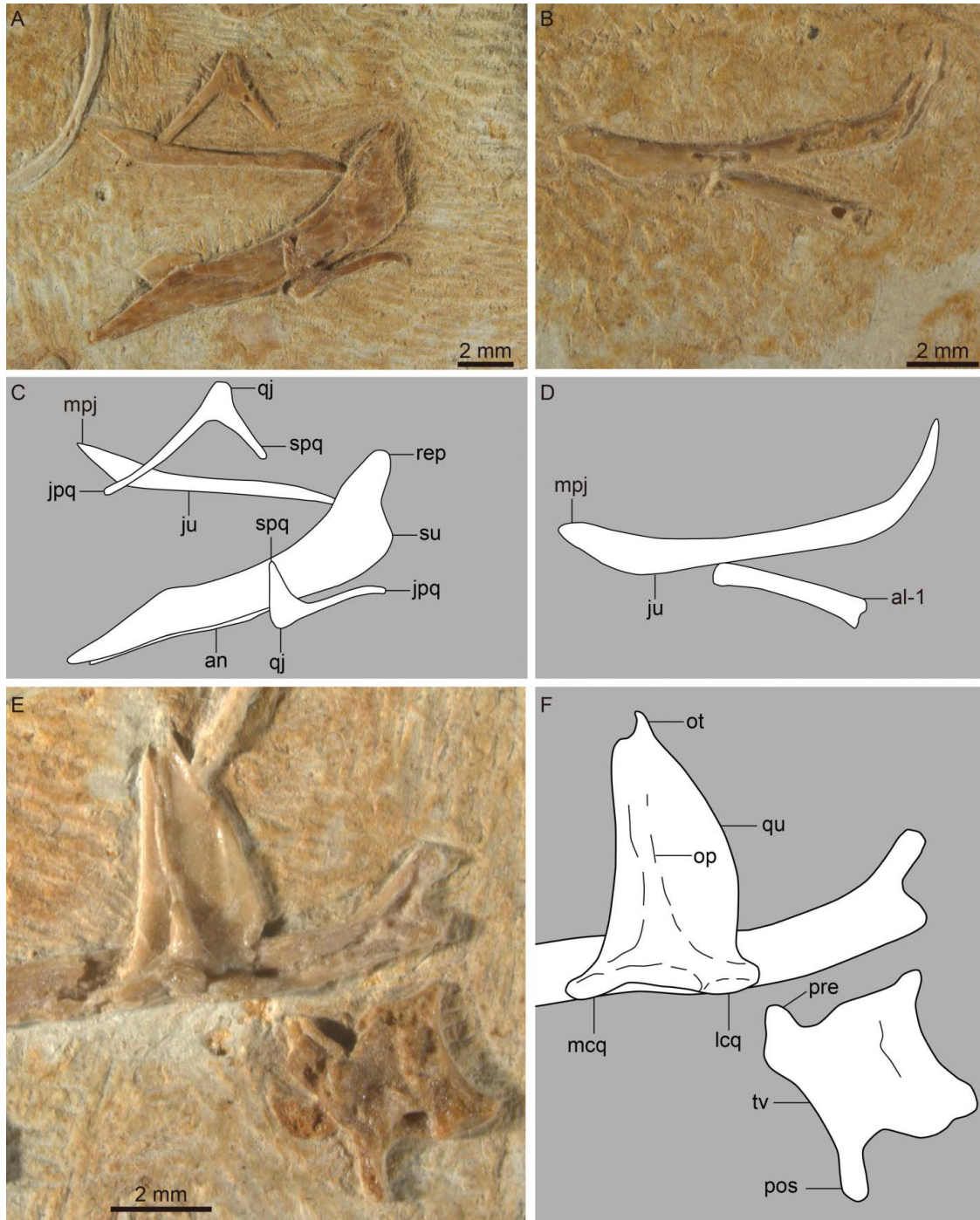


Figure 3. Cranial elements of *Pterygornis dapingfangensis* gen. et sp. nov. (IVPP V20729). **A–D**, jugal and quadrate; **E, F**, right quadrate in rostral view. Abbreviations: al-1, the first phalanx of alular digit; an, angular; jpq, jugal process of quadrate; ju, jugal; lcq, lateral condyle of quadrate; mcq, medial condyle of quadrate; mpj, maxillary process of jugal; op, orbital process of quadrate; ot, otic process of quadrate; pre, prezygapophysis; pos, postzygapophysis; qp, quadrate; qu, quadrate; rep, retroarticular process; spq, squamosal process of quadrate; su, surangular; tv, thoracic vertebra.

The tooth is subconical and has a slightly caudally curved occlusal tip. The left surangular is preserved in lateral view (Fig. 3). The bone is robust with straight dorsal and ventral margins. The rostral end of the surangular slopes

rostroventrally, a condition unknown amongst enantiornithines, in which the rostral end slants rostrorodorsally to accommodate the distal end of the dentary which is caudoventrally tapered (O'Connor & Chiappe 2011). The odd

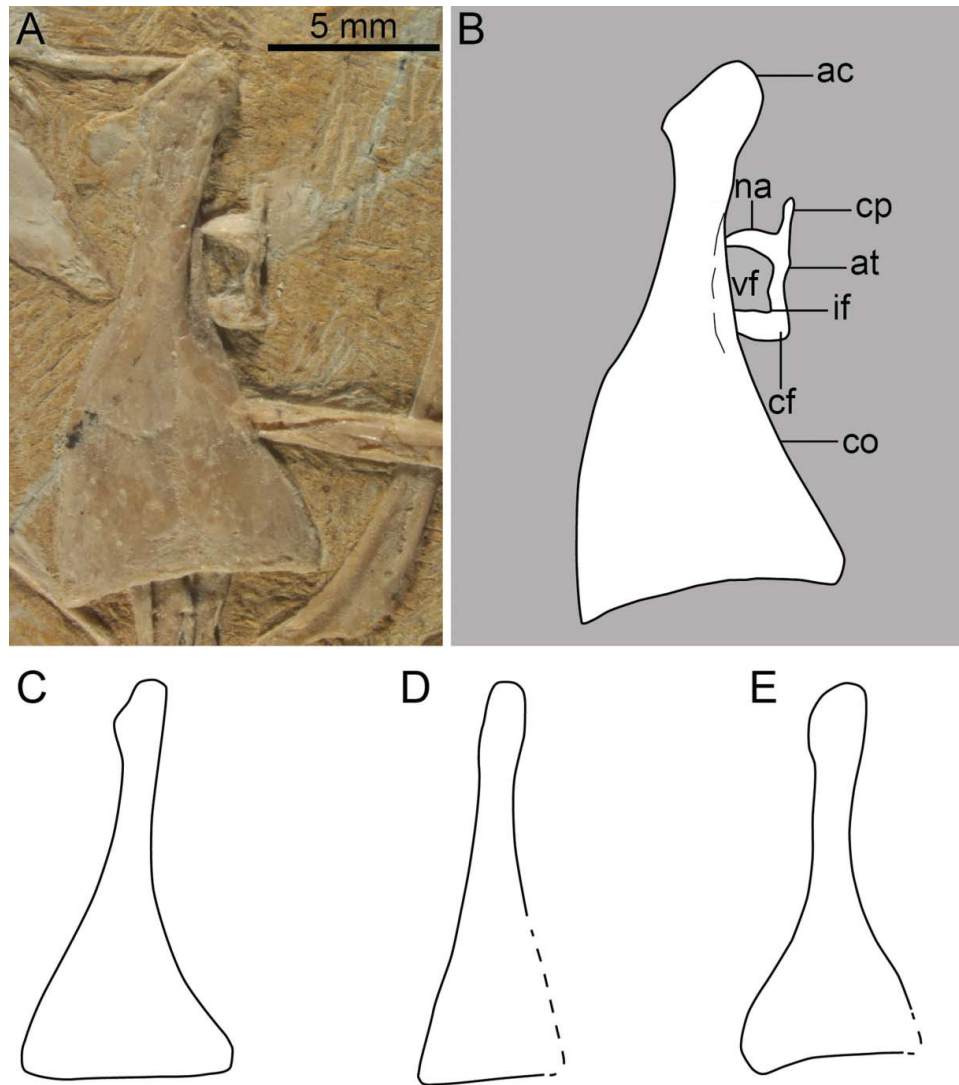


Figure 4. Photograph and line drawing of the atlas and the right coracoid of *Pterygornis dapingfangensis* gen. et sp. nov. (IVPP V20729) and the coracoids of selected enantiornithines. **A, B**, *Pterygornis dapingfangensis*; **C**, *Eoenantiornis buhleri*; **D**, *Vescornis hebeiensis*; **E**, *Shenqiornis mengi*. Line drawings in C–E are transformed to the right coracoid in cranial view, and are not to scale. Abbreviations: ac, acroracoid process; at, atlas; cf, condyloid fossa; co, coracoid; cp, costal process; if, incisura fossae; na, neural arch; vf, vertebral foramen.

morphology of the rostral end of the surangular indicates that the dentary and surangular do not articulate via a suture contact but in an overlapping manner in some enantiornithines. No coronoid process is developed, as in many enantiornithines with a few exceptions, including *Rapaxavis pani*, *L. kurochkini* and *Fortunguavis xiaotaizicus* (O'Connor *et al.* 2011; Wang *et al.* 2014a, c). Caudally, a caudodorsally directed retroarticular process is developed as in STM11-80 (Wang *et al.* in press). The angular is thin and rod-like, firmly articulating with the ventral margin of the surangular. The splenial is preserved in its entirety (Figs 1, 2). Due to imperfect preservation, the morphology of this bone can only be observed in a few taxa amongst enantiornithines. As in *Vescornis hebeiensis*, the splenial is

triangular with a long rostral ramus and a short caudal ramus (Zhang *et al.* 2004). The ventral margin is straight, but the dorsal margin slopes ventrally from its dorsal apex towards both extremities. An isolated bone close to the left nasal is tentatively interpreted as the palatine (Fig. 1). The palatal elements are usually poorly preserved amongst enantiornithines, particularly in the Jehol specimens that are often more or less crushed, making their morphology equivocal. The bone's morphology resembles that of the palatine of *Gobipteryx minuta* in that it is composed of a wide paddle-like lamina and a slender rod-like portion (Chiappe *et al.* 2001). If our interpretation is correct, then the lamina represents the maxillary process and the rod-like portion represents the pterygoid wing.

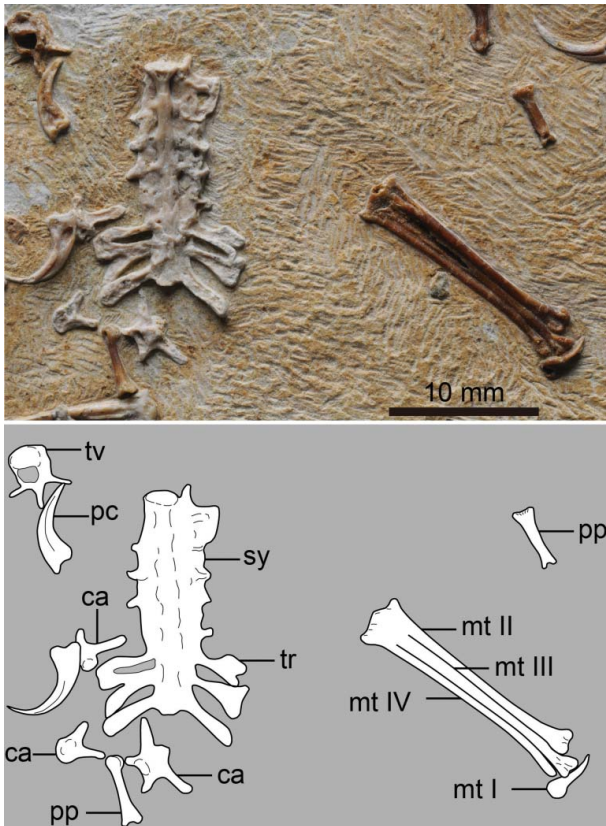


Figure 5. Photograph and line drawing of the synsacrum and the left tarsometatarsus of *Pterygornis dapingfangensis* gen. et sp. nov. (IVPP V20729). Abbreviations: ca, caudal vertebra; mt I–IV, metatarsal I–IV; pc, pedal claw; pp, pedal phalanx; sy, synsacrum; tr, transverse process; tv, thoracic vertebra.

Axial skeleton

The vertebral column is disarticulated and incomplete. Eight cervical vertebrae are recognized including the atlas and axis. The atlas is preserved in cranial view, and its left portion is overlain by the right coracoid (Fig. 4). Due to poor preservation, the morphology of the atlas has only been described in the holotypes of *Pengornis houi* (IVPP V15336) and *Zhouornis hani* (CNUVB-0903) amongst enantiornithines (Zhou *et al.* 2008; Zhang *et al.* 2013). As in these two taxa, and living birds, the bone is ring-like. The neural arch is fused to the centrum. The dorsolateral portion of the neural arch is wide and laminar, and the arch narrows ventrally. A small process projecting laterally from the arch is interpreted as the costal process, also present in *P. houi* (see Zhou *et al.* 2008, fig. 3b); however, this feature is lacking in *Z. hani* and most living birds (Baumel & Witmer 1993). The condyloid fossa is concave and faces craniodorsally, receiving the occipital condyle of the skull. As in some living birds (e.g. *Struthio camelus* and *Meleagris gallapavo*), the condyloid fossa is excavated dorsally by the incisura fossae (Baumel & Witmer 1993; Livezey & Zusi 2006). Therefore, the vertebral foramen is rounded with sharply constricted ventral

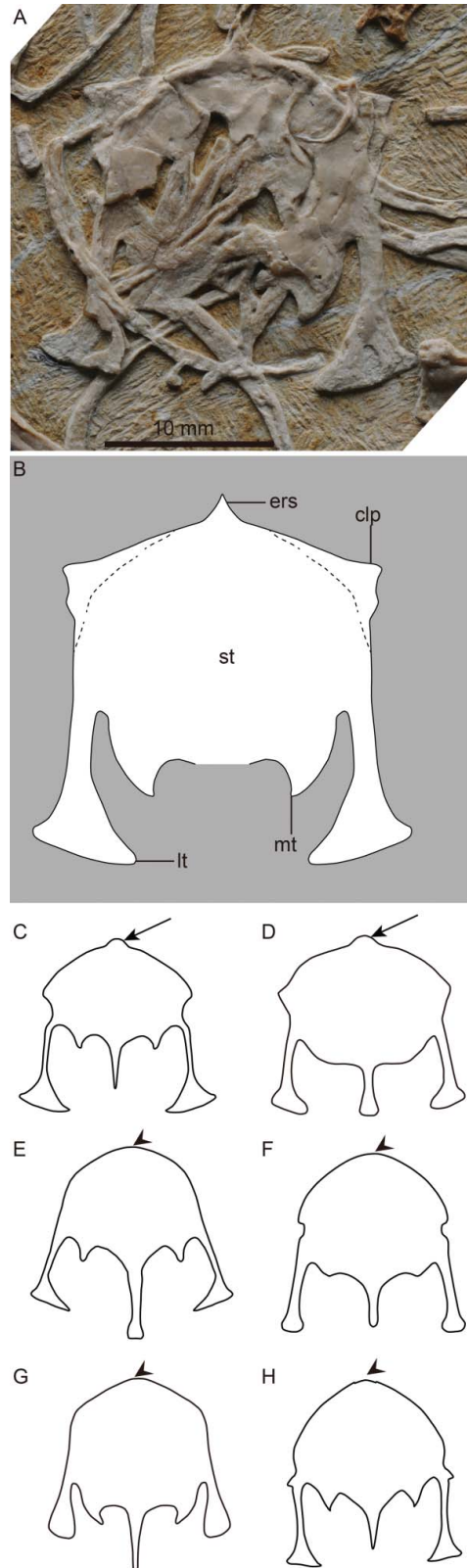


Figure 6. Sternal morphology of *Pterygornis dapingfangensis* gen. et sp. nov. in comparison with other enantiornithines. **A, B**, holotype of *Pterygornis dapingfangensis* (IVPP V20729); **C**, *Houornis caudatus* (modified from Wang & Liu 2015); **D**,

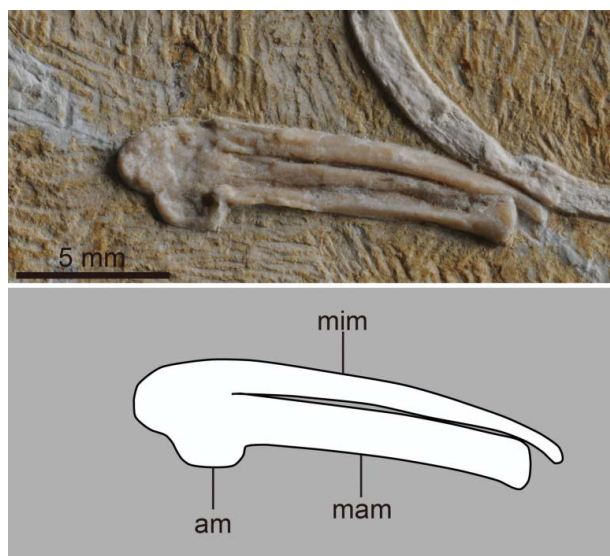


Figure 7. Photograph and line drawing of the left carpometacarpus (dorsal view) of *Pterygornis dapingfangensis* gen. et sp. nov. (IVPP V20729). Abbreviations: am, alular metacarpal; mam, major metacarpal; mim, minor metacarpal.

margin. Unfortunately, the corresponding area is overlain by the odontoid process in the *Z. hani* holotype, and is poorly preserved in the *P. houi* holotype. A short ventral process is evident, but it is absent in *Z. hani* (see Zhang *et al.* 2013, fig. 3); whether it is present in *P. houi* cannot be ascertained due to the poor preservation. The axis is preserved in craniodorsal view and displaced close to the right radius (Fig. 1). The prezygapophyses project less cranially than the odontoid process, and the postzygapophyses are well developed.

The preserved postaxial cervical vertebrae are approximately equal in length and width. The cranial articular facet is heterocoelous, but the condition of the caudal articular facet is obscured by preservation. The cervical rib and transverse process are ankylosed to form the enclosed transverse foramen. The spinous process is absent. The postzygapophyses are longer than the prezygapophyses and project caudally beyond the associated centrum by a distance that is about half the centrum length; the epipophyses are located on the postzygapophyses and fail to reach their distal margins.

Eocathayornis walkeri; **E**, *Parabohaiornis martini* (modified from Wang *et al.* 2014a); **F**, *Longipteryx chaoyangensis* **G**, *Eoenantiornis buhleri*; **H**, *Cathayornis yandica* (modified from Wang & Liu 2015). Arrows in C and D indicate the rostral spine, but whether it is the external or internal cannot be determined due to preservation; arrow heads in E and H show that the rostral spine is absent in many other enantiornithines, e.g. *P. martini*, *L. chaoyangensis*, *E. buhleri* and *C. yandica*. Line drawings in C–H are not to scale. Abbreviations: clp, cranial process; ers, external rostral spine; lt, lateral trabecula; mt, medial trabecula; st, sternum.

Table 1. Selected measurements of the holotype of *Pterygornis dapingfangensis* gen. et sp. nov., IVPP V20729.

Element	Length (mm)
Pygostyle	12.3
Coracoid	15.9
Humerus	25.3
Ulna	28.3
Radius	26.4
Alular metacarpal	2.4
Carpometacarpus	13.3
Alular digit 1	4.4
Major digit 1	7.1
Femur	23.8
Tibiotarsus	28.6
Fibula	12.2
Metatarsal II	15.1
Metatarsal III	17.0
Metatarsal IV	15.6

Seven thoracic vertebrae are discernible (Figs 1, 2). The centrum is longer than wide. The spinous process is tall, exceeding the height of associated vertebral foramen. Both the cranial and caudal articular facets are amphicoelous. The vertical height of the cranial articular facet is greater than half that of the vertebral foramen. A prominent ventral process is present, approaching the height of the spinous process. The centrum is excavated laterally by a broad depression and the parapophysis is centrally located, both conditions characteristic of Enantiornithes (Chiappe & Walker 2002).

The synsacrum is composed of eight ankylosed sacral vertebrae, more than in *Iberomesornis romeralis* (five), *Rapaxavis pani* (six or seven) and *Protopteryx fengningensis* (seven) (Zhang & Zhou 2000; Sereno *et al.* 2002; O'Connor *et al.* 2011). The bone is exposed in ventral view (Fig. 5). The cranial vertebral articulation of the first sacral vertebra is deeply concave, and is wider than high, whereas the caudal articular surface of the synsacrum is convex. The prezygapophyses of the first sacral vertebra project further cranially than its centrum. The transverse processes of the cranial five sacral vertebrae are short, possibly truncated by postmortem crush, and are coalesced by the transverse lamina. Comparatively, the transverse processes of the caudal three vertebrae are elongated and becoming increasingly caudally directed, as in other enantiornithines (Wang *et al.* 2014c).

Six free caudal vertebrae are preserved (Figs 1, 5). Enantiornithes typically have six to eight free caudals (Sanz *et al.* 2002; O'Connor *et al.* 2011; Wang *et al.* 2014b, c), and thus it is impossible to determine if additional caudals were present in the complete skeleton. The transverse processes are caudolaterally directed, and are

longer than their associated centrum width. The prezygapophyses project cranially beyond the cranial articular facet, whereas the postzygapophyses are absent. As in living birds (e.g. *Pucrasia macrolopha*), the spinous process is forked at its dorsal end. The pygostyle is fully ankylosed, with its constituent vertebrae indistinguishable. The bone is in lateral view and exhibits the dorsal and ventrolateral processes, as is typical of most other enantiornithines (Chiappe & Walker 2002). The dorsal process is restricted cranially, whereas the ventrolateral process extends nearly along the entire length of the pygostyle. The ribs are scattered in the slab (Fig. 1).

Pectoral girdle

Both coracoids are exposed in cranial view. The coracoid is strut-like and lacks the procoracoid process (Fig. 5). As is the typical condition of enantiornithines, the lateral margin is convex and the medial margin is concave (Chiappe & Walker 2002). The strongly convex lateral margin makes the omal end of the coracoid strongly curved medially as in *Cathayornis yandica*, *Eocathayornis walkeri* and Enantiornithes indet. CAGS-IG-02-0901 (Zhou 2002; Zhou & Hou 2002; You *et al.* 2005), whereas the omal end is straight in other Jehol enantiornithines, including *Eoenantiornis buhleri* and *Vescornis hebeiensis* (Fig. 4). The coracoid expands rapidly from the rod-like neck and forms the broad sternal end. The sternal margin is concave, and the sternolateral process is not developed. A medial groove runs along the medial margin of the neck; however, whether a supracoracoidal nerve foramen is present and opens into this groove, as in other enantiornithines (Chiappe & Walker 2002; O'Connor 2009), cannot be determined due to preservation.

The scapulae are straight, lacking the sagittally curved condition reported in some enantiornithines, including *Fortunguavis xiaotaizicus*, *Zhouornis hani* and *Dunhuangia cuii* (Zhang *et al.* 2013; Wang *et al.* 2014a, 2015). Although the proximal end is largely overlain by other elements, a broad acromion is present and strongly projects dorsally.

The sternum is nearly complete except the xiphial region (Fig. 6). The sternal body is nearly quadrangular. Cranially, a small process projects from the middle of the cranial margin of the sternum, and is continuous laterally with the external labra of the coracoidal sulci, indicating that it is homologous to the external rostral spine of modern birds (Baumel & Witmer 1993). A similar structure is otherwise known only in *Houornis caudatus* and *E. walkeri* amongst enantiornithines; however, the poor preservation makes it unclear whether it is the external or the internal rostral spine in the latter two taxa (Wang & Liu 2015). A pair of craniolateral processes is developed which are broad and triangular. The craniolateral processes have so far been reported only in *Concornis*

lacustris and possibly *Rapaxavis pani* within enantiornithines (Sanz *et al.* 2002; Zheng *et al.* 2012). As is typical of enantiornithines, the caudal end of the sternum is notched by two pairs of trabeculae. The lateral trabecula is robust, with a fan-shaped distal expansion as in *Houornis caudatus* and *C. yandica*. However, *C. yandica* bears a short process extending from the proximal end of the lateral trabecula (Wang & Liu 2015), but this feature is absent in IVPP V20729. The medial trabecula is short, robust and triangular and curves medially, resembling that of *Bohaiornis guoi* (Wang *et al.* 2014c).

Thoracic limbs

The left and right humeri are exposed in caudal and cranial view, respectively (Fig. 1). The proximal margin of the humerus is concave centrally, bounded by proximal convexities dorsally and ventrally, a synapomorphy of Enantiornithes (Chiappe & Walker 2002). The cranial surface of the bicipital crest is poorly preserved, and thus a pit-shaped fossa reported in some enantiornithines cannot be determined (Chiappe & Walker 2002; Walker *et al.* 2007). Caudally, the ventral tubercle is well projected, and separated from the caudal convexity of the humeral head by a deep capital incision. There is no evidence of a pneumotricipital foramen on the proximocaudal surface, indicating that a diverticulum of the clavicular air sac penetrating the humerus as in living birds is lacking (Chiappe & Walker 2002). As in many other Jehol enantiornithines, the deltopectoral crest is narrow and projects dorsally, without cranial deflection. The flexor process protrudes well distally, making the distal surface of the humerus proximodorsally angled. The dorsal and ventral condyles are cranially located, and the ventral one is poorly preserved. As in most other enantiornithines, the caudal surface of the distal end of the humerus is nearly flat and lacks both humerotricipital and scapulotricipital grooves (Chiappe & Walker 2002; Wang & Liu 2015).

The ulna is slightly longer than the humerus. The bone is bowed over the proximal half, but straight distally. The bicipital tubercle and the brachial impression are apparently lacking. The olecranon process is weakly developed. The dorsal and ventral cotylae are adjacent and nearly flat. As in other enantiornithines and more basal birds, quill knobs for the attachment of the secondary remiges are absent (Chiappe *et al.* 1999; Chiappe & Walker 2002; Zhou & Zhang 2003; Wang *et al.* 2014c). The radius is straight and bears a longitudinal groove on its interosseous surface of the proximal half shaft, a condition characteristic of enantiornithines (Chiappe & Walker 2002). The ulnare is nearly rectangular and exhibits a shallow metacarpal incision. The radiale is square-shaped and smaller than the ulnare.

The left carpometacarpus is exposed in dorsal view (Fig. 7). Proximally, the major and minor metacarpals are

fused to each other and also to the semilunate carpal. The alular metacarpal is completely fused to the major metacarpal as in some Late Cretaceous enantiornithines (Walker & Dyke 2009). In contrast, this bone, although ankylosed proximally, is not fused to the major metacarpal distally in all known Early Cretaceous enantiornithines. The alular metacarpal has a straight cranial margin, indicating that an extensor process is absent. The major metacarpal is rectangular. The minor metacarpal extends distally beyond the major metacarpal, as is typical of enantiornithines (Chiappe & Walker 2002). The minor metacarpal becomes craniocaudally compressed distally, and firmly articulates with rather than being fused to the caudal surface of the major metacarpal. A faint intermetacarpal space is developed and is much narrower than the midshaft width of the minor metacarpal. The manual phalanges are disarticulated and incomplete. Two elements close to the left femur are interpreted as the first phalanges of the major and alular digits, based on comparisons with complete hands of other enantiornithines. The first phalanx of the major digit lacks the craniocaudal expansion reported in ornithuromorphs; the bone constricts just proximal to its distal articular facet, as in *Sulcavis georum* and *Dunhuangia cuii* (O'Connor *et al.* 2013b; Wang *et al.* 2015). The first phalanx of the alular digit is slender and shorter than that of the major digit. No pelvic elements are preserved.

Pelvic limbs

The left and right femora are exposed in cranial and medial aspects, respectively. The shaft is slightly bowed craniocaudally and measures about 83% the length of the tibiotarsus. The femoral head projects medially and is situated on a short neck. The trochanteric crest extends proximally to the level of the femoral head; comparatively, it projects further proximally in *Fortunguavis xiaotaizicus* and *Martinavis* sp. (Walker & Dyke 2009; Wang *et al.* 2014a). The proximal tarsals are fused to the tibia. Both tibiotarsi are preserved in caudal view. The shaft slightly expands at the proximal and distal ends. The fibular crest extends for the proximal third of the tibiotarsus. The proximal end of the fibula is transversely compressed. The bone rapidly tapers distally to a slender split.

The distal tarsals are fused to the proximal ends of three major metatarsals, but metatarsals II–IV are unfused distally, a condition known in most enantiornithines and more basal birds (Chiappe *et al.* 1999; Chiappe & Walker 2002; Zhou & Zhang 2003; Wang 2014). Both tarsometatarsi are exposed in plantar view. Metatarsal V is absent (Fig. 5). The proximal articular surface of the tarsometatarsus is wider than the combined widths of metatarsals II–IV at the proximal end, and bears a low intercotylar prominence. The shaft of the tarsometatarsus rapidly narrows below the proximal margin and expands

mediolaterally when it approaches the trochleae. In plantar view, there is no evidence of a caudal projection or groove on the proximocaudal surface, indicating that the hypotarsus of Neornithes is lacking. The proximal two-thirds of metatarsals II and IV bear plantar projections, rendering the plantar surface of the tarsometatarsus excavated. Distally, the plantar projections of metatarsals II and IV are reduced, and the plantar surface of the tarsometatarsus is nearly flat. Metatarsal III is the longest, closely followed by metatarsal IV, and metatarsal II extends to the proximal margin of the metatarsal III trochlea. Metatarsals II and IV are approximately of the same width; as in other enantiornithines (Chiappe & Walker 2002), metatarsal IV is thinner and its trochlea is reduced to a single condyle. The metatarsal II trochlea is considerably wider than that of metatarsal III, whereas these trochleae are subequal in width in some enantiornithines, such as *Houornis caudatus* and *Rapaxavis pani*. The metatarsal II trochlea has a well-formed ginglymoid articulation, and a wide articular furrow is visible on its planar surface. The lateral rim of the trochlea projects distally slightly beyond the medial rim, reminiscent of but to a lesser degree than in *Vescornis hebeiensis* and *F. xiaotaizicus*. Proximal to the trochlea, the plantar surface of metatarsal II lacks the fossa for metatarsal I. On its distal end, the medial rim of the metatarsal III trochlea extends further proximally and plantarly than the lateral rim; the lateral rim is transversely wider. Both metatarsals I are preserved. The bone is straight in lateral view (the right one), and P-shaped in craniolateral view (the left one) with a mediocaudally deflected distal end for articulation with the hallux. The pedal digits are disarticulated, making it impossible to determine their assignments. The non-ungual phalanges are spool-shaped with well-developed pits for the attachment of the collateral ligament. The unguals are recurved and laterally excavated by distinct neurovascular sulci.

Discussion

Comparison and phylogenetic analysis

IVPP V20729 is referable to Enantiornithes by sharing the following synapomorphies with this diverse clade: the lateral margin of the coracoid is convex; the proximal margin of the humerus is concave centrally, and rises dorsally and ventrally; the radius bears a longitudinal groove on its interosseous surface; the minor metacarpal projects further distally than the major metacarpal; the pygostyle develops a pair of ventrolateral processes; and metatarsal IV is thinner than metatarsals II and III (Chiappe & Walker 2002). Compared with other equal-sized enantiornithines, IVPP V20729 is uniquely similar to *Houornis caudatus* and *Eocathayornis walkeri* in having a rostral spine of the sternum. In IVPP V20729, this structure can

be identified as the external rostral spine, but whether it is the external or the internal one cannot be ascertained in *H. caudatus* and *E. walkeri* due to preservation (Wang & Liu 2015). A similar structure is so far unreported in other enantiornithines (Zheng *et al.* 2012; Wang 2014). However, the sternum of IVPP V20729 differs from that of *H. caudatus* and *E. walkeri* in having a pair of cranio-lateral processes (Fig. 6). This feature is otherwise known only in *Concornis lacustris* and possibly *Rapaxavis pani* amongst enantiornithines (Sanz *et al.* 2002; O'Connor *et al.* 2011). IVPP V20729 differs from these two taxa in a number of morphological features. In *C. lacustris* (Sanz *et al.* 2002), the cranio-lateral processes project from the proximal end of the lateral trabecula, more caudally positioned relative to that of IVPP V20729; in addition, metatarsals II and IV are subequal in length in *C. lacustris*, but metatarsal IV extends further distally in IVPP V20729. *Rapaxavis pani* is characterized by a suite of features, e.g. the sternal lateral trabecula is forked distally, the manual digits are reduced and the pygostyle is constricted distally (O'Connor *et al.* 2011). All these features are absent in the new specimen. The complete fusion of the compound bones, particularly that the alular metacarpal is fused to the major metacarpal, and the smooth bone surface, indicate that the specimen was adult at the time of death. Therefore, the preserved morphologies are not subject to further ontogenetic variations. The unique sternal morphology distinguishes the new specimen from the known enantiornithines, supporting the erection of a new taxon, *Pteryornis dapingfangensis* gen. et sp. nov.

The fully ankylosed alular and major metacarpals in *P. dapingfangensis* are unique and warrant further discussion. The fusion of these two bones is functionally beneficial for powered flight, because the ankylosed alular metacarpal would have stabilized the alular digit, which serves the attachment of the bastard wing – a critical structure for slow flight and manoeuvrability (Thomas 1993). However, these two bones are only fused proximally in other known Early Cretaceous enantiornithines, and complete fusion is only present in Late Cretaceous forms (Chiappe & Walker 2002; O'Connor 2009; Wang *et al.* 2014c). One possible explanation is that the fusion between the alular and carpometacarpus completes considerably late amongst Early Cretaceous enantiornithines such that no specimens ever reached this ontogenetic status. However, numerous specimens consistently lack this feature, particularly individuals with apparent adult osteological marks, e.g. all bone epiphyses are ossified, fused tibiotarsus and tarsometatarsus, and fusion of the cervical ribs to enclose transverse foramina, making this interpretation implausible. Noticeably, the pelvic elements are unfused in all known Early Cretaceous enantiornithines, but are ankylosed in Late Cretaceous taxa (Chiappe & Walker 2002; Walker & Dyke 2009). All these observations suggest that there is a general increase in the degree

of fusion in compound bones during the evolution of Enantiornithes, and that the lack of fusion between the alular and the major metacarpals in most Early Cretaceous specimens is not resultant from ontogeny. Therefore, we propose that the complete fusion of alular and metacarpals represents an autapomorphy of *P. dapingfangensis*.

To determine the relationship of *P. dapingfangensis* relative to other enantiornithines, we performed a phylogenetic analysis using the data matrix modified from Wang *et al.* (2014c; see Methods and Online Supplementary Material). The phylogenetic analysis produced 370 most parsimonious trees (MPTs) of 1046 steps, and an additional round of TBR search yielded 768 MPTs of equal length. The strict consensus tree is largely resolved and places *P. dapingfangensis* in a derived position within Enantiornithes (Fig. 8). The new topology is generally consistent with recent studies regarding the placements of the major clades (Zhou *et al.* 2014a, b; O'Connor & Zhou 2013; Wang *et al.* 2014c, 2015). In Enantiornithes, a large polytomy composed of *P. fengningensis*, the Pengornithidae and Longipterygidae is resolved in a more basal position relative to other enantiornithines. The recently established clades, including the Pengornithidae, Longipterygidae and Bohaiornithidae, were recovered here (O'Connor *et al.* 2009; Wang *et al.* 2014c; Wang *et al.* 2014), but the interrelationships within the latter two clades were incompletely resolved. *Cathayornis yandica*, *E. walkeri* and *P. dapingfangensis* form the consecutive outgroups to a small polytomy consisting of *Vescornis hebeiensis*, *Neuquenornis volans*, *Gobipteryx minuta*, *Ealulavis hoyasi* and the clade [*Qiliania graffini* + *C. lacustris*]. Ornithuromorpha is well resolved. As in previous studies, *Archaeorhynchus spathula* was recovered as the basalmost ornithuromorph (O'Connor & Zhou 2013; Wang *et al.* 2014c). The recently described *Iteravis hunchzemeyeri* emerged in a more derived position than other Jehol birds, corroborating the previous result that *I. hunchzemeyeri* represents the most derived known Jehol ornithuromorph (Zhou *et al.* 2014b).

Implications for early evolution of avian cranial morphology

The known skull materials of Enantiornithes are largely from the Jehol Biota, with a few reports from the Early Cretaceous of Spain and the Late Cretaceous of Argentina and Mongolia. The skull remains from Mongolia are mostly referred to *Gobipteryx minuta*, and are preserved in three dimensions but largely incomplete (Elzanowski 1977; Chiappe *et al.* 2001); and recently, Kurochkin *et al.* (2013) reported an embryonic enantiornithine from Mongolia with poorly preserved cranial bones. For skull material from Argentina, only one specimen, the holotype of *Neuquenornis volans*, preserves the frontal, parietal and occipital bones (Chiappe & Calvo 1994). The skull

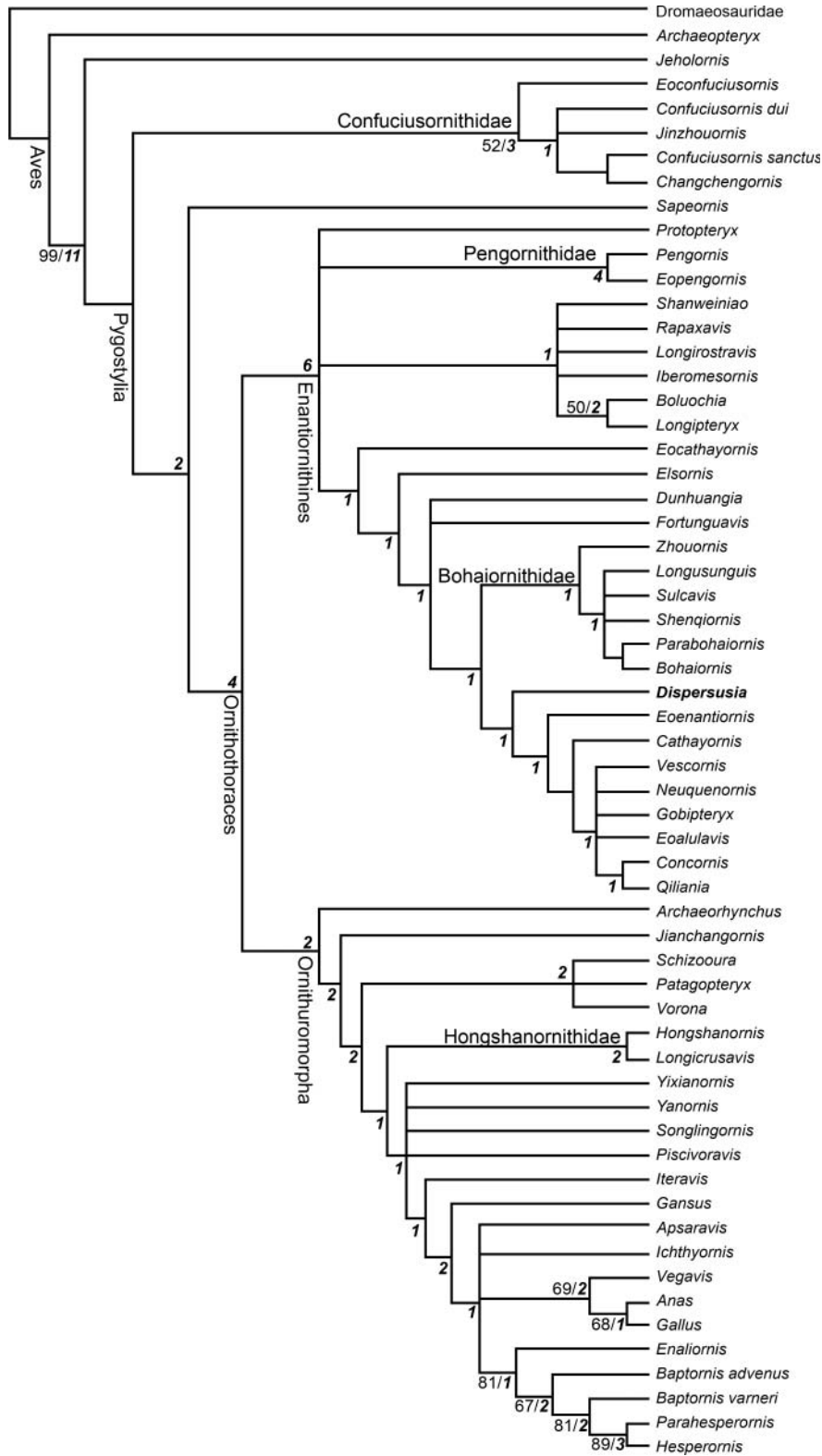


Figure 8. Cladogram showing the phylogenetic position of *Pterygornis dapingfangensis* gen. et sp. nov. amongst Mesozoic birds. Bootstrap and Bremer values are indicated to the corresponding nodes in normal and bold italic formats, respectively.

material from Spain is represented by a single specimen (Enantiornithes indet. LP4450), which is preserved in similar condition to the Jehol birds (Sanz *et al.* 1997). The Jehol enantiornithines are usually complete and articulated. Unfortunately, the known Jehol enantiornithines are mostly crushed and preserved primarily in two dimensions. Consequently, the gracile cranial elements are overlapping and compressed, severely limiting the number of morphological features that can be discerned. Therefore, detailed cranial morphology remains largely unknown for enantiornithines. However, the cranial bones of IVPP V20729 are disarticulated and well preserved, allowing a rare chance to reconstruct the morphology of certain cranial elements, particularly the jugal and quadratojugal bones.

The jugal is usually described as an arched rod-like element in enantiornithines, but the morphology of its caudal end can only be observed in a few taxa, including *Shenqiornis mengi*, *Longsunguis kurochkini*, *Bohaiornis guoi*, *Cathayornis yandica* and Enantiornithes indet. LP4450, and exhibits noticeable variations. As in *L. kurochkini* and *C. yandica*, the caudal end of the jugal in the new bird is unforked, tapered and dorsally curved (Figs 3, 9; Wang *et al.* 2014c; Wang & Liu 2015). In contrast, it is bifurcated into the postorbital and quadratojugal processes in *S. mengi* and Enantiornithes indet. LP4450 (O'Connor & Chiappe 2011). The forked condition is widely distributed in non-ornithothoracine birds, including *Archaeopteryx bavarica*, *Jeholornis prima*, *Confuciusornis sanctus* and

Sapeornis chaoyangensis (Fig. 9; Elzanowski & Wellnhofer 1996; Chiappe *et al.* 1999; Zhou & Zhang 2002, 2003), but the jugal is more robust than in enantiornithines. Interestingly, the forked jugal is also reported in a basal ornithuromorph *Schizooura lii* but absent in sympatric ornithuromorph *Yixianornis grabau* (Clarke *et al.* 2006; Zhou *et al.* 2012). The forked condition in these early birds is reminiscent of non-avian dinosaurs, but considerably reduced, in which the postorbital and the jugal processes are heavily built and elongated (Fig. 9; Paul 1988; Currie & Zhao 1993; Xu & Wu 2001; Norell *et al.* 2006).

Typically, the postorbital process in non-avian dinosaurs contacts the jugal process of the postorbital, which together separate the orbit completely from the infratemporal fenestra (Barsbold & Osmolska 1999; Weishampel *et al.* 2004; Xu *et al.* 2004, 2015). In basal birds such as *A. bavarica* and Early Cretaceous taxa, the gracile postorbital process of the jugal may have failed to contact the postorbital (Chiappe *et al.* 1999; Elzanowski 2002; O'Connor & Chiappe 2011), although well-preserved specimens are needed to test this hypothesis. In living birds, the postorbital process of the jugal and the postorbital are absent (Baumel & Witmer 1993; Livezey & Zusi 2006). These findings indicate that the forked morphology represents a plesiomorphic condition and that some enantiornithines evolved the unforked jugal morphology in parallel with ornithuromorphs.

The quadratojugal has only been briefly mentioned in one enantiornithine. In the holotype of *Eocathayornis*

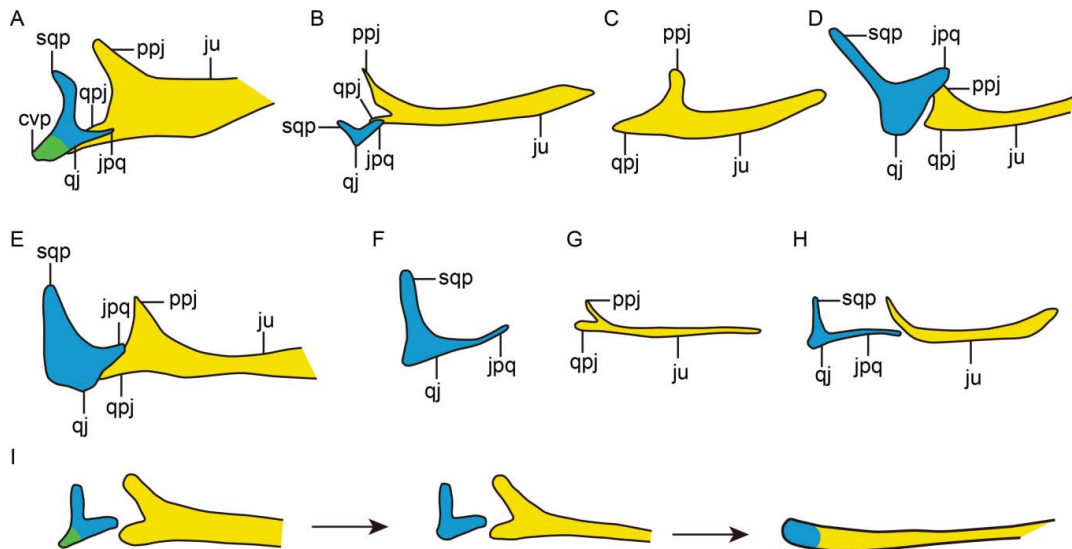


Figure 9. Jugal and quadratojugal in dromaeosaurid and basal birds. **A**, *Linheraptor exquisitus* (IVPP V16923); **B**, the seventh skeleton of *Archaeopteryx* (modified from Elzanowski & Wellnhofer 1996); **C**, *Jeholornis prima* (IVPP V13274); **D**, *Sapeornis chaoyangensis* (IVPP V13275); **E**, *Confuciusornis sanctus* (modified from Chiappe *et al.* 1999); **F**, *Archaeorhynchus spathula* (IVPP V14287); **G**, *Schizooura lii* (IVPP V16861); **H**, *Pterygornis dapingfangensis* (IVPP V20729); **I**, hypothetical morphological modifications of jugal–quadratojugal in dinosaur–bird transition: the caudoventral and squamosal processes of the quadratojugal reduced sequentially (from T-shaped to L-shaped), and finally fused to the jugal in more advanced birds; and the caudal end of jugal is changed from forked to unforked condition. Abbreviations: cvp, caudoventral process of quadratojugal; jpq, jugal process of quadratojugal; ju, jugal; ppj, postorbital process of jugal; qj, quadratojugal; qpj, quadratojugal process of jugal; sqp, squamosal process of the quadratojugal.

walkeri, a short bone caudal to the jugal is tentatively interpreted as the quadratojugal by Zhou (2002). Regardless of whether the quadratojugal is correctly identified in this study, anatomical features of this element still remain unknown. In *Pterygornis dapingfangensis*, the quadratojugal is an inverted L-shaped element with jugal and squamosal processes (Figs 3, 9). Both processes are slender and splint-like, and the jugal process is longer. Similar morphology is also visible in *A. bavarica*, *S. chaoyangensis*, *C. sanctus* and *Archaeorhynchus spathula* (Fig. 9; Elzanowski & Wellnhofer 1996; Martin *et al.* 1998; Zhou & Zhang 2006a; Martin 2010). By contrast, amongst the closest relatives of birds such as the dromaeosaurids, the bone is shaped like an inverted T with a distinct caudoventral processes extending from the caudal end of the quadratojugal (Fig. 9; Paul 1988; Xu & Wu 2001; Norell *et al.* 2006). This process is reduced and the caudal end of the quadratojugal is blunt in *A. bavarica* and Early Cretaceous birds (Elzanowski & Wellnhofer 1996; Martin *et al.* 1998; Zhou & Zhang 2003, 2006a). In basal birds such as *A. bavarica* and Early Cretaceous forms, the squamosal process of the quadratojugal is short and delicate, possibly failing to contact the squamosal (Martin *et al.* 1998; Elzanowski 2002), whereas in dromaeosaurids the process is stout and long, which contacts the quadratojugal process of the squamosal, forming a completely delimited infra-temporal fenestra (Paul 1988; Xu & Wu 2001; Xu *et al.* 2015). In living birds, the quadratojugal is fused to the jugal before hatching, and the fused jugal bar is unforked caudally (Baumel & Witmer 1993; Maxwell 2008a, b). Therefore, all these observations reveal that the quadratojugal underwent large modifications with the reduction of the caudoventral and squamosal processes sequentially during early avian evolution (Fig. 9).

The large modifications in jugal and quadratojugal reflect the refined cranial kinesis in basal birds relative to their dinosaurian ancestors. Modern birds characteristically have a kinetic skull in which the upper jaw or a part of it can be moved with respect to the brain case, which is significant in the feeding behaviour (Zusi 1993). Such a functional property involves a complicated mechanism and the refinement of the cranial elements (Zusi 1984). Compared with non-avian dinosaurs, the most conspicuous modifications in cranial elements pertaining to the skull kinesis of modern birds are the absence of the postorbital, and of the squamosal–quadratojugal and the jugal–postorbital articulations, which enable the quadrate to rotate rostrocaudally, pushing the jugal bar and the pterygoid–palate bar forward or backward; in turn, the rostrum can be elevated or depressed with respect to the brain case (Chiappe *et al.* 1999, 2002). The reduced squamosal process of the quadratojugal and the postorbital process of the jugal in *P. dapingfangensis* and more basal birds indicate that refinement for cranial kinesis occurred early in avian evolution. However, it is still unclear whether the squamosal–quadratojugal

and/or the jugal–postorbital articulations are completely lost in Early Cretaceous birds due to imperfect preservation, which is critical to our knowledge regarding the evolution of cranial kinesis of modern birds.

Acknowledgements


We thank Jie Zhang for taking the photographs. We are grateful to two anonymous reviewers for their constructive comments for improving the manuscript. This project was funded by the National Science Foundation for Fostering Talents in Basic Research of the National Natural Science Foundation of China (J1210008), the National Basic Research Program of China (973 Program, 2012CB821906) and the National Natural Science Foundation of China (41172020).

Supplemental material

Supplemental material for this article can be accessed at: <http://dx.doi.org/10.1080/14772019.2015.1073801>

ORCID

Min Wang  <http://orcid.org/0000-0001-8506-1213>

Han Hu  <http://orcid.org/0000-0001-5926-7306>

References

- Barsbold, R. & Osmolska, H. 1999. The skull of *Velociraptor* (Theropoda) from the Late Cretaceous of Mongolia. *Acta Palaeontologica Polonica*, **44**, 189–219.
- Baumel, J. J. & Witmer, L. M. 1993. Osteologia. Pp. 45–132 in J. J. Baumel, A. S. King, J. E. Breazile, H. E. Evans & J. C. Vanden Berge (eds) *Handbook of avian anatomy: nomina anatomica avium*. 2nd edition. Nuttall Ornithological Club, Cambridge.
- Benton, M. J., Zhou, Z., Orr, P. J., Zhang, F. & Kearns, S. L. 2008. The remarkable fossils from the Early Cretaceous Jehol Biota of China and how they have changed our knowledge of Mesozoic life. *Proceedings of the Geologists' Association*, **119**, 209–228.
- Chiappe, L. M. 1995. The phylogenetic position of the Cretaceous birds of Argentina: Enantiornithes and *Patagopteryx deferrariisi*. *Courier Forschungsinstitut Senckenberg*, **181**, 55–63.
- Chiappe, L. M. & Calvo, J. O. 1994. *Neuquenornis volans*, a new Late Cretaceous bird (Enantiornithes: Avisauridae) from Patagonia, Argentina. *Journal of Vertebrate Palaeontology*, **14**, 230–246.
- Chiappe, L. M. & Walker, C. A. 2002. Skeletal morphology and systematics of the Cretaceous Euenantiornithes (Ornithothoraces: Enantiornithes). Pp. 240–267 in L. M. Chiappe & L. M. Witmer (eds) *Mesozoic birds: above the heads of dinosaurs*. University of California Press, Berkeley.

- Chiappe, L. M., Ji, S., Ji, Q. & Norell, M. A.** 1999. Anatomy and systematics of the Confuciusornithidae (Theropoda: Aves) from the Late Mesozoic of northeastern China. *Bulletin of the American Museum of Natural History*, **242**, 1–89.
- Chiappe, L. M., Norell, M. & Clark, J.** 2001. A new skull of *Gobipteryx minuta* (Aves: Enantiornithes) from the Cretaceous of the Gobi Desert. *American Museum Novitates*, **3346**, 1–15.
- Chiappe, L. M., Norell, M. & Clark, J.** 2002. The Cretaceous, short-armed Alvarezsauridae: *Mononykus* and its kin. Pp. 87–120 in L. M. Chiappe & L. M. Witmer (eds) *Mesozoic birds: above the heads of dinosaurs*. University of California Press, Berkeley.
- Clarke, J. A., Zhou, Z. & Zhang, F.** 2006. Insight into the evolution of avian flight from a new clade of Early Cretaceous ornithurines from China and the morphology of *Yixianornis grabaui*. *Journal of Anatomy*, **208**, 287–308.
- Currie, P. J. & Zhao, X.** 1993. A new carnosaur (Dinosauria, Theropoda) from the Jurassic of Xinjiang, People's Republic of China. *Canadian Journal of Earth Sciences*, **30**, 2037–2081.
- Elzanowski, A.** 1977. Skulls of *Gobipteryx* (Aves) from the Upper Cretaceous of Mongolia. *Acta Palaeontologica Polonica*, **37**, 153–165.
- Elzanowski, A.** 2002. Archaeopterygidae (Upper Jurassic of Germany). Pp. 240–267 in L. M. Chiappe & L. M. Witmer (eds) *Mesozoic birds: above the heads of dinosaurs*. University of California Press, Berkeley.
- Elzanowski, A. & Wellnhofer, P.** 1996. Cranial morphology of *Archaeopteryx*: evidence from the seventh skeleton. *Journal of Vertebrate Palaeontology*, **16**, 81–94.
- Goloboff, P. A., Farris, J. S. & Nixon, K. C.** 2008. *TNT: tree analysis Using New Technology, vers. 1.1 (Willi Hennig Society Edition)*. Program and documentation available at <http://www.zmuc.dk/public/phylogeny/tnt>.
- He, H., Wang, X., Zhou, Z., Wang, F., Boven, A., Shi, G. & Zhu, R.** 2004. Timing of the Jiufotang Formation (Jehol Group) in Liaoning, northeastern China, and its implications. *Geophysical Research Letters*, **31**, L12605.
- He, H., Wang, X., Jin, F., Zhou, Z., Wang, F., Yang, L., Ding, X., Boven, A. & Zhu, R.** 2006. The $^{40}\text{Ar}/^{39}\text{Ar}$ dating of the early Jehol Biota from Fengning, Hebei Province, northern China. *Geochemistry, Geophysics, Geosystems*, **7**, Q04001.
- Howard, H.** 1929. The avifauna of Emeryville shell mound. *University of California Publications in Zoology*, **32**, 301–394.
- Jin, F., Zhang, F., Li, Z., Zhang, J., Li, C. & Zhou, Z.** 2008. On the horizon of *Protopteryx* and the early vertebrate fossil assemblages of the Jehol Biota. *Chinese Science Bulletin*, **53**, 2820–2827.
- Kurochkin, E. N., Chatterjee, S. & Mikhailov, K. E.** 2013. An embryonic enantiornithine bird and associated eggs from the Cretaceous of Mongolia. *Paleontological Journal*, **47**, 1252–1269.
- Linnaeus, C.** 1758. *Systema naturae per regna tria naturae, secundum classes, ordines, genera, species, cum characteribus, differentiis, synonymis, locis. Volume I*, Regnum Animale. Editio decima, reformata. Laurentii Salvii, Stockholm, 824 pp.
- Livezey, B. C. & Zusi, R. L.** 2006. Higher-order phylogeny of modern birds (Theropoda, Aves: Neornithes) based on comparative anatomy: I. Methods and characters. *Bulletin of Carnegie Museum of Natural History*, **37**, 1–544.
- Longrich, N. R., Tokaryk, T. & Field, D. J.** 2011. Mass extinction of birds at the Cretaceous-Paleogene (K-Pg) boundary. *Proceedings of the National Academy of Sciences*, **108**, 15253–15257.
- Martin, L. D.** 2010. The other half of avian evolution: Cyril Walker's contribution. *Journal of Systematic Palaeontology*, **9**, 3–8.
- Martin, L. D., Zhou, Z., Hou, L. & Feduccia, A.** 1998. *Confuciusornis sanctus* compared to *Archaeopteryx lithographica*. *Naturwissenschaften*, **85**, 286–289.
- Maxwell, E. E.** 2008a. Comparative embryonic development of the skeleton of the domestic turkey (*Meleagris gallopavo*) and other galliform birds. *Zoology*, **111**, 242–257.
- Maxwell, E. E.** 2008b. Ossification sequence of the avian order anseriformes, with comparison to other precocial birds. *Journal of Morphology*, **269**, 1095–1113.
- Norell, M. A., Clark, J. M., Turner, A. H., Makovicky, P. J., Barsbold, R. & Rowe, T.** 2006. A new dromaeosaurid theropod from Ukhaa Tolgod (Ömnögovi, Mongolia). *American Museum Novitates*, **3345**, 1–51.
- O'Connor, J. K.** 2009. *A systematic review of Enantiornithes (Aves: Ornithothoraces)*. Unpublished PhD thesis, University of Southern California, Los Angeles, 600 pp.
- O'Connor, J. K. & Chiappe, L. M.** 2011. A revision of enantiornithine (Aves: Ornithothoraces) skull morphology. *Journal of Systematic Palaeontology*, **9**, 135–157.
- O'Connor, J. K. & Zhou, Z.** 2013. A redescription of *Chaoyangia beishanensis* (Aves) and a comprehensive phylogeny of Mesozoic birds. *Journal of Systematic Palaeontology*, **11**, 889–906.
- O'Connor, J. K., Wang, X., Chiappe, L. M., Gao, C., Meng, Q., Cheng, X. & Liu, J.** 2009. Phylogenetic support for a specialized clade of Cretaceous enantiornithine birds with information from a new species. *Journal of Vertebrate Paleontology*, **29**, 188–204.
- O'Connor, J. K., Chiappe, L. M., Gao, C. & Zhao, B.** 2011. Anatomy of the Early Cretaceous enantiornithine bird *Rapaxavis pani*. *Acta Palaeontologica Polonica*, **56**, 463–475.
- O'Connor, J. K., Zheng, X., Wang, X., Wang, Y. & Zhou, Z.** 2013a. Ovarian follicles shed new light on dinosaur reproduction during the transition towards birds. *National Science Review*, **1**, 15–17.
- O'Connor, J. K., Zhang, Y., Chiappe, L. M., Meng, Q., Li, Q. & Liu, D.** 2013b. A new enantiornithine from the Yixian Formation with the first recognized avian enamel specialization. *Journal of Vertebrate Paleontology*, **33**, 1–12.
- Pan, Y., Sha, J., Zhou, Z. & Fürsich, F.** 2013. The Jehol Biota: definition and distribution of exceptionally preserved relicts of a continental Early Cretaceous ecosystem. *Cretaceous Research*, **44**, 30–38.
- Paul, G.** 1988. The small predatory dinosaurs of the mid-Mesozoic: the horned theropods of the Morrison and Great Oolite—*Ornitholestes* and *Proceratosaurus*—and the sickle-claw theropods of the Cloverly, Djadokhta and Judith River—*Deinonychus*, *Velociraptor* and *Saurornitholestes*. *Hunteria*, **2**, 1–9.
- Sanz, J. L., Chiappe, L. M., Pérez-Moreno, B. P., Moratalla, J. J., Hernández-Carrasquilla, F., Buscalioni, A. D., Ortega, F., Poyato-Ariza, F. J., Rasskin-Gutman, D. & Martínez-Delellós, X.** 1997. A nestling bird from the Lower Cretaceous of Spain: implications for avian skull and neck evolution. *Science*, **276**, 1543–1546.
- Sanz, J. L., Pérez-Moreno, B. P., Chiappe, L. M. & Buscalioni, A.** 2002. The birds from the Lower Cretaceous of Las Hoyas (Province of Cuenca, Spain). Pp. 209–229 in L. M. Chiappe & L. M. Witmer (eds) *Mesozoic birds: above the heads of dinosaurs*. University of California Press, Berkeley.

- Sereno, P. C., Rao, C. & Li, J.** 2002. *Sinornis santensis* (Aves: Enantiornithes) from the Early Cretaceous of Northeastern China. Pp. 184–208 in L. M. Chiappe & L. M. Witmer (eds) *Mesozoic birds: above the heads of dinosaurs*. University of California Press, Berkeley.
- Thomas, A. L. R.** 1993. On the aerodynamics of birds' tails. *Transactions of the Royal Society of London, Series B*, **340**, 361–380.
- Turner, A. H., Pol, D., Clarke, J. A., Erickson, G. M. & Norell, M.** 2007. A basal dromaeosaurid and size evolution preceding avian flight. *Science*, **317**, 1378–1381.
- Walker, C. A.** 1981. New subclass of birds from the Cretaceous of South America. *Nature*, **292**, 51–53.
- Walker, C. A. & Dyke, G. J.** 2009. Euenantiornithine birds from the Late Cretaceous of El Brete (Argentina). *Irish Journal of Earth Sciences*, **27**, 15–62.
- Walker, C. A., Buffetaut, E. & Dyke, G. J.** 2007. Large euenantiornithine birds from the Cretaceous of southern France, North America and Argentina. *Geological Magazine*, **144**, 977–986.
- Wang, M.** 2014. *Taxonomical revision, ontogenetic, habitat and phylogenetic analyses of Enantiornithes (Aves: Ornithothoraces) of China*. Unpublished PhD thesis, University of Chinese Academy of Sciences, 464 pp.
- Wang, M. & Liu, D.** 2015. Taxonomical reappraisal of Cathayornithidae (Aves: Enantiornithes). *Journal of Systematic Palaeontology*, doi: 10.1080/14772019.2014.994087.
- Wang, M., O'Connor, J. K. & Zhou, Z.** 2014a. A new robust enantiornithine bird from the Lower Cretaceous of China with scansorial adaptations. *Journal of Vertebrate Paleontology*, **34**, 657–671.
- Wang, M., Zhou, Z. & Xu, G.** 2014b. The first enantiornithine bird from the Upper Cretaceous of China. *Journal of Vertebrate Paleontology*, **34**, 135–145.
- Wang, M., Zhou, Z., O'Connor, J. K. & Zelenkov, N. V.** 2014c. A new diverse enantiornithine family (Bohaiornithidae fam. nov.) from the Lower Cretaceous of China with information from two new species. *Vertebrata Palasiatica*, **52**, 31–76.
- Wang, M., Li, D., O'Connor, J. K., Zhou, Z. & You, H.** 2015. Second species of enantiornithine bird from the Lower Cretaceous Changma Basin, northwestern China with implications for the taxonomic diversity of the Changma avifauna. *Cretaceous Research*, **55**, 56–65.
- Wang, X., O'Connor, J. K., Zheng, X., Wang, M., Hu, H. & Zhou, Z.** 2014. Insights into the evolution of rachis dominated tail feathers from a new basal enantiornithine (Aves: Ornithothoraces). *Biological Journal of Linnean Society*, **113**, 805–819.
- Wang, Y., Wang, M., O'Connor, J. K., Wang, X., Zheng, X. & Zhang, X.** in press. A new Jehol enantiornithine bird with three dimensional preservation and ovarian follicles. *Journal of Vertebrate Paleontology*.
- Weishampel, D. B., Dodson, P. & Osmolska, H.** 2004. *The Dinosauria*. 2nd edition. University of California Press, Berkeley, 880 pp.
- Xu, X. & Wu, X.** 2001. Cranial morphology of *Sinornithosaurus millenii* Xu et al. 1999 (Dinosauria: Theropoda: Dromaeosauridae) from the Yixian Formation of Liaoning, China. *Canadian Journal of Earth Sciences*, **38**, 1739–1752.
- Xu, X., Norell, M. A., Kuang, X., Wang, X., Zhao, Q. & Jia, C.** 2004. Basal tyrannosauroids from China and evidence for protofeathers in tyrannosauroids. *Nature*, **431**, 680–684.
- Xu, X., Pittman, M., Sullivan, C., Choiniere, J., Tan, Q., Clark, J., Norell, A. & Wang, S.** 2015. The taxonomic status of the Late Cretaceous dromaeosaurid *Linheraptor exquiritus* and its implications for dromaeosaurid systematics. *Vertebrata Palasiatica*, **53**, 29–62.
- You, H., O'Connor, J. K., Chiappe, L. M. & Ji, Q.** 2005. A new fossil bird from the Early Cretaceous of Gansu Province, northwestern China. *Historical Biology*, **17**, 7–14.
- Zhang, F. & Zhou, Z.** 2000. A primitive enantiornithine bird and the origin of feathers. *Science*, **290**, 1955–1959.
- Zhang, F., Ericson, P. G. P. & Zhou, Z.** 2004. Description of a new enantiornithine bird from the Early Cretaceous of Hebei, northern China. *Canadian Journal of Earth Sciences*, **41**, 1097–1107.
- Zhang, F., Zhou, Z. & Dyke, G. J.** 2006. Feathers and 'feather-like' integumentary structures in Liaoning birds and dinosaurs. *Geological Journal*, **41**, 395–404.
- Zhang, Z., Chiappe, L. M., Han, G. & Chinsamy, A.** 2013. A large bird from the Early Cretaceous of China: new information on the skull of enantiornithines. *Journal of Vertebrate Paleontology*, **33**, 1176–1189.
- Zheng, X., Martin, L. D., Zhou, Z., Burnham, D. A., Zhang, F. & Miao, D.** 2011. Fossil evidence of avian crops from the Early Cretaceous of China. *Proceedings of the National Academy of Sciences*, **108**, 15904–15907.
- Zheng, X., Wang, X., O'Connor, J. K. & Zhou, Z.** 2012. Insight into the early evolution of the avian sternum from juvenile enantiornithines. *Nature Communications*, **3**, 1116.
- Zheng, X., O'Connor, J. K., Huchzermeyer, F., Wang, X., Wang, Y., Wang, M. & Zhou, Z.** 2013. Preservation of ovarian follicles reveals early evolution of avian reproductive behaviour. *Nature*, **495**, 507–511.
- Zheng, X., O'Connor, J. K., Wang, X., Wang, X., Zhang, X. & Zhou, Z.** 2014. On the absence of sternal elements in *Anchiornis* (Paraves) and *Sapeornis* (Aves) and the complex early evolution of the avian sternum. *Proceedings of the National Academy of Sciences*, **111**, 13900–13905.
- Zhou, S., Zhou, Z. & O'Connor, J. K.** 2012. A new basal beaked Ornithurine bird from the Lower Cretaceous of western Liaoning, China. *Vertebrata Palasiatica*, **50**, 9–24.
- Zhou, S., Zhou, Z. & O'Connor, J. K.** 2014a. A new piscivorous ornithuromorph from the Jehol Biota. *Historical Biology*, **26**, 608–618.
- Zhou, S., O'Connor, J. K. & Wang, M.** 2014b. A new species from an ornithuromorph (Aves: Ornithothoraces) dominated locality of the Jehol Biota. *Chinese Science Bulletin*, **59**, 5366–5378.
- Zhou, Z.** 2002. A new and primitive enantiornithine bird from the Early Cretaceous of China. *Journal of Vertebrate Paleontology*, **22**, 49–57.
- Zhou, Z.** 2014. The Jehol Biota, an Early Cretaceous terrestrial Lagerstätte: new discoveries and implications. *National Science Review*, **1**, 543–559.
- Zhou, Z. & Hou, L.** 2002. The discovery and study of Mesozoic birds in China. Pp. 160–183 in L. M. Chiappe & L. M. Witmer (eds) *Mesozoic birds: above the heads of dinosaurs*. University of California Press, Berkeley.
- Zhou, Z. & Zhang, F.** 2002. A long-tailed, seed-eating bird from the Early Cretaceous of China. *Nature*, **418**, 405–409.
- Zhou, Z. & Zhang, F.** 2003. Anatomy of the primitive bird *Sapeornis chaoyangensis* from the Early Cretaceous of Liaoning, China. *Canadian Journal of Earth Sciences*, **40**, 731–747.
- Zhou, Z. & Zhang, F.** 2006a. Mesozoic birds of China—a synoptic review. *Vertebrata Palasiatica*, **44**, 74–98.
- Zhou, Z. & Zhang, F.** 2006b. A beaked basal ornithurine bird (Aves, Ornithurae) from the Lower Cretaceous of China. *Zoologica Scripta*, **35**, 363–373.

- Zhou, Z. & Wang, Y.** 2010. Vertebrate diversity of the Jehol Biota as compared with other Lagerstätten. *Science China Earth Sciences*, **53**, 1894–1907.
- Zhou, Z., Barrett, P. M. & Hilton, J.** 2003. An exceptionally preserved Lower Cretaceous ecosystem. *Nature*, **421**, 807–814.
- Zhou, Z., Chiappe, L. M. & Zhang, F.** 2005. Anatomy of the Early Cretaceous bird *Eoenantiornis buhleri* (Aves: Enantiornithes) from China. *Canadian Journal of Earth Sciences*, **42**, 1331–1338.
- Zhou, Z., Clarke, J. & Zhang, F.** 2008. Insight into diversity, body size and morphological evolution from the largest Early Cretaceous enantiornithine bird. *Journal of Anatomy*, **212**, 565–577.
- Zusi, R. L.** 1984. A functional and evolutionary analysis of rynchokinesis in birds. *Smithsonian Contributions to Zoology*, **395**, 1–40.
- Zusi, R. L.** 1993. Patterns of diversity in the avian skull. Pp. 391–437 in J. Hanken & B. K. Hall (eds) *The skull*. University of Chicago Press, Chicago.